THE JOURNAL OF PHYSICAL CHEMISTRY Letters

Letter

pubs.acs.org/JPCL

Activating Carrier Multiplication in PbSe Quantum Dot Solids by Infilling with Atomic Layer Deposition

Sybren ten Cate,[†] Yao Liu,[‡] C. S. Suchand Sandeep,[†] Sachin Kinge,[§] Arjan J. Houtepen,[†] Tom J. Savenije,[†] Juleon M. Schins,[†] Matt Law,[‡] and Laurens D. A. Siebbeles*[,†]

[†]Optoelectronic Materials Section, Department of Chemical Engineering, Delft University of Technology, Julianalaan 136, 2628 BL Delft, The Netherlands

[‡]Department of Chemistry, University of California, Irvine, Irvine, California 92697, United States

[§]Toyota Europe, Materials Research & Development, Hoge Wei 33, B-1930 Zaventem, Belgium

Supporting Information

ABSTRACT: Carrier multiplication—the generation of multiple electron–hole pairs by a single photon—is currently of great interest for the development of highly efficient photovoltaics. We study the effects of infilling PbSe quantum-dot solids with metal oxides by atomic layer deposition on carrier multiplication. Using time-resolved microwave conductivity measurements, we find, for the first time, that carrier multiplication occurs in 1,2-ethanedithiol-linked PbSe quantum-dot solids infilled with Al_2O_3 or Al_2O_3/ZnO, while it is negligible or absent in noninfilled films. The carrier-multiplication efficiency of the infilled quantum-dot solids is close to that of solution-dispersed PbSe quantum dots, and not significantly limited by Auger recombination.

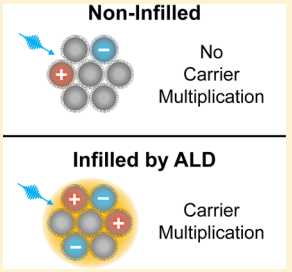

SECTION: Physical Processes in Nanomaterials and Nanostructures

Colloidal semiconductor quantum dots (QDs) currently receive a great deal of interest for applications in photovoltaics.[1−3] This is due to their tunable band gap, cheap solution-based synthesis and processing, and, most promisingly, the occurrence of carrier multiplication (CM; also called multiple exciton generation),[4−9] where the absorption of one photon of sufficiently high energy results in the generation of multiple electron–hole pairs of lower energy. In the presence of CM, the optimal band gap for harvesting the solar spectrum shifts from 1.34 eV (Shockley–Queisser limit: no CM) to 0.7 eV (ideal CM).[6,9,10] Lead chalcogenide QDs have a band gap tunable over this range,[11] which makes them ideal candidates for utilizing CM in photovoltaics. CM has been observed for PbSe QDs in dispersion.[4,12−14]

In thin-film QD solids for photovoltaic applications, QDs are electronically coupled by replacing the bulky passivating ligands used during synthesis by shorter molecules. In this way, band gap tunability is maintained, and charge mobility is increased due to the decreased width of inter-QD tunneling barriers.[15,16] Applications suffer from the rapid degradation in air of such films because the short linker molecules provide almost no protection against oxidation.[17] Recently, infilling the interstitial space of 1,2-ethanedithiol-linked PbSe (PbSe-EDT) QD solids with inorganic matrices (Al_2O_3 or Al_2O_3 followed by ZnO) by atomic layer deposition (ALD) was shown to produce air-stable films by suppressing oxidative and photo–thermal degradation of the QDs.[17,18] Furthermore, infilling PbSe-EDT QD solids enhances charge mobility by up to an order of magnitude, attributed to a passivation of charge trap states.[18]

Here we investigate the yield of multiple free electrons and holes that result from CM in PbSe-EDT QD solids infilled with Al_2O_3 or Al_2O_3 followed by ZnO. Note that this multiple free charge generation (MFCG) yield is not necessarily the same as the CM yield. CM leads to the generation of multiple electrons and holes that initially reside in close proximity. These charges can undergo Auger recombination unless they quickly move away from each other. The MFCG yield is determined by the extent to which the latter occurs. MFCG thus requires both CM and a subsequent escape of charges from Auger recombination. We find that ALD infilling activates the MFCG efficiency: from weak or absent before infilling, due to negligible CM,[19−21] to approaching the intrinsic CM efficiency reported for isolated PbSe QDs in dispersion.[4] Infilling is thus an important technique for the realization of cheap, robust CM-enhanced photovoltaics.

Three infilled PbSe-EDT QD solids were prepared (6.3 nm QD diameter; see Methods section). One QD solid was infilled with Al_2O_3, a second with Al_2O_3(1 nm)/ZnO(5 nm) (i.e., 1 nm of Al_2O_3 followed by 5 nm of ZnO), and a third with Al_2O_3(3 nm)/ZnO(5 nm). The films were then overcoated with 20–30 nm Al_2O_3 to guarantee their stability in air. The resulting QD solids have a band gap energy of 0.64 eV (λ = 1930 nm) and retain quantum confinement on infilling (cf. Figure S1, Supporting Information). A noninfilled PbSe-EDT QD solid (6.0 nm QD diameter) was studied as a control.

Received: April 8, 2013
Accepted: May 8, 2013

   dx.doi.org/10.1021/jz4007492 | J. Phys. Chem. Lett. 2013, 4, 1766–1770

The charge mobility of the QD solids was determined by time-resolved microwave conductivity measurements (TRMC; see Methods),[22,23] similar to a previous study on films of PbSe QDs with 1,2-ethanediamine ligands.[24] The samples were mounted in a microwave cavity (8.5 GHz resonance frequency) and excited with a 3 ns laser pulse of tunable wavelength. Photogeneration of mobile charge carriers leads to absorption of microwave power. The latter can be related to the product of the mobility μ and yield of mobile charge carriers per incident photon η, summed for photogenerated electrons and holes: $\eta_e(t)\mu_e + \eta_h(t)\mu_h$; see Methods. Figure 1 shows typical

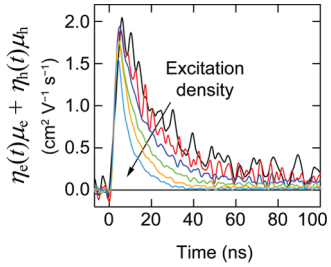

Figure 1. Effect of varying photoexcitation density on charge decay in an Al_2O_3-infilled PbSe-EDT QD solid. The vertical axis displays the product of the mobility μ and yield of mobile charge carriers per incident photon η, summed for photogenerated electrons and holes: $\eta_e(t)\mu_e + \eta_h(t)\mu_h$ (see Methods). Photoexcitation (λ = 500 nm, i.e., hν = 3.9E_g) was performed with a density varied from 2 × 10^{-4} to 6 × 10^{-2} photons per QD.

microwave conductivity transients for photoexcitation of the Al_2O_3-infilled PbSe-EDT QD solid at varying excitation density. The signal initially rises due to the generation of mobile charges during the laser pulse, reaches a maximum at time $t = t_{max}$ and subsequently decays due to first-order processes or higher-order Auger recombination of electrons and holes. Auger recombination becomes faster at higher excitation density, as expected, and it becomes negligible for photoexcitation densities below 2 × 10^{-4} photons per QD (see Methods). The decay kinetics are independent of photoexcitation energy at low excitation density. The noninfilled PbSe-EDT QD solid behaves similarly (data not shown).

The yield of mobile charge carriers per incident photon, η, is proportional to the magnitude of the transients as shown in Figure 1. The latter was determined at sufficiently low excitation density so that nongeminate charge recombination does not play a role within the 3 ns time resolution. The results are displayed in Figure 2 (red symbols, left axis) together with the fraction of absorbed photons, F_A (black curve, right axis), as a function of photon energy. The curve of η follows the shape of the low-energy absorption peak (due to the $1S_h1S_e$ transition), implying a constant quantum yield of free charges per absorbed photon, $\phi \equiv \eta/F_A$, for this transition. At higher photon energies η increases faster than the fraction of absorbed photons, F_A, implying an increase of the quantum yield, ϕ.

Figure 3 shows the quantum yield, ϕ, for the Al_2O_3-infilled PbSe-EDT QD solid, normalized to the mean value in the interval $(1.75–2.70)E_g$. Photoexcitation of the $1S_h1S_e$ and $1P_h1P_e$ transitions ($h\nu \leq 1.25E_g$) gives an identical quantum yield to within experimental uncertainty. For photon energy in the range $(1.25–1.75)E_g$ the quantum yield undergoes a sigmoid rise centered at the third electronic transition. Since CM is energetically forbidden at these energies, this implies that third-transition electron–hole pairs more easily lead to

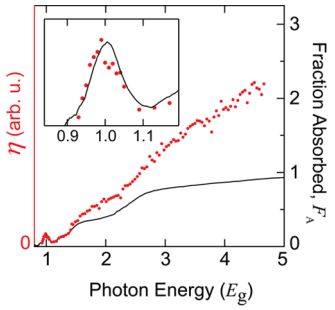

Figure 2. Action spectrum of the Al_2O_3-infilled PbSe-EDT QD solid. The left axis shows the yield of mobile charge carriers per incident photon: η, which is proportional to $\eta_e(t = t_{max})\mu_e + \eta_h(t = t_{max})\mu_h$. The right axis shows the fraction of incident photons absorbed by the sample, F_A. The horizontal axis displays $h\nu/E_g$, with E_g the band gap energy of the QD solid (determined from Figure S1). The yield of mobile charge carriers per incident photon increases more strongly with photon energy than F_A does. Inset: for excitation near the band gap, the yield is proportional to F_A.

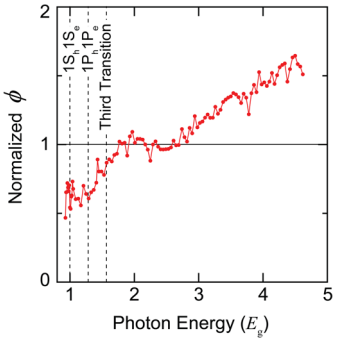

Figure 3. Normalized quantum yield versus band gap normalized photon energy for the Al_2O_3-infilled PbSe-EDT QD solid. The quantum yield, ϕ, is the yield of free charges per absorbed photon: $\phi \equiv \eta/F_A$. The first three electronic transitions of the film are indicated by dashed lines (see Note 1, Supporting Information). The normalized quantum yield saturates to unity at $1.75E_g$, and MFCG occurs with threshold energy $2.70E_g$.

mobile charges than $1S_h1S_e$ or $1P_h1P_e$ pairs. Such an effect has been observed previously in devices of noninfilled PbSe-EDT QD solids, and was tentatively attributed to the production of more trapped excitons at lower photon energy.[21] It could also be that electron–hole pairs of the third transition and higher have a larger spatial delocalization, thus increasing the effective distance between electron and hole and decreasing the Coulomb attraction. For photoexcitation in the range $(1.75–2.70)E_g$, the quantum yield shows no further increase with photon energy. This is likely due to a saturation of the dissociation yield at unity, a value as reported for a 1,2-ethanediamine (EDA)-linked PbSe QD solid excited at $1.75E_g$.[25]

For photoexcitation above a threshold energy $h\nu_{th} = 2.70E_g$, the quantum yield increases with photon energy. This is attributed to MFCG (note: carrier mobility is independent of excitation energy since hot charges thermally relax within the present time resolution).[26] It has an associated MFCG efficiency of 0.35 ± 0.01 (standard deviation), quantified by the slope for $h\nu \geq 2.70E_g$ in Figure 3: $\Delta\phi/\Delta(h\nu/E_g)$, analogous to the CM efficiency as defined in the literature.[27] While CM has not been observed for noninfilled PbSe-EDT QD solids (cf.

dx.doi.org/10.1021/jz4007492 | J. Phys. Chem. Lett. 2013, 4, 1766–1770

Figure 4),[19−21] the present results show for the first time that infilling leads to the generation of free charges by CM.

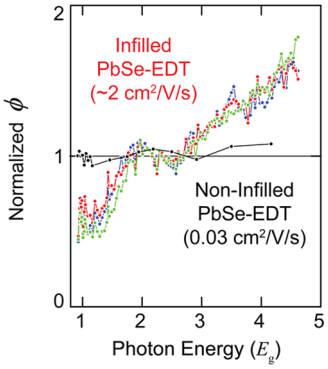

Figure 4. Infilled PbSe-EDT QD solids exhibit a significant effect of CM on the charge yield, in contrast to a noninfilled sample. Results for PbSe-EDT QD solids: noninfilled (black), infilled with Al_2O_3 (red), infilled with Al_2O_3(1 nm)/ZnO(5 nm) (blue), and infilled with Al_2O_3(3 nm)/ZnO(5 nm) (green).

Effects of infilling on the efficiency of charge carrier generation via CM were investigated by comparing results for three differently infilled PbSe-EDT QD solids to that of the noninfilled PbSe-EDT QD solid (see Figure 4). Note that the quantum yield values were normalized to their mean value in the interval $(1.75-2.70)E_g$, as in Figure 3. The quantum yield for the noninfilled PbSe-EDT QD solid (black symbols, Figure 4) shows no effects of CM, in agreement with earlier findings for noninfilled PbSe-EDT QD solids.[19−21] However, in contrast to earlier device measurements[21] and in contrast to the three infilled QD solids, it does not increase on going from the $1S_h1S_e$ and $1P_h1P_e$ transitions to the third electronic transition. The reason for this difference is unclear, but is outside the scope of the present work.

The dependence of the yield of mobile charge carriers on photon energy is seen to be similar for the differently infilled films, with the MFCG efficiency being equal to 0.35 ± 0.03. This is close to the 0.41 CM efficiency measured for isolated PbSe QDs in dispersion on a picosecond time scale prior to Auger recombination,[4] which occurs within ~100 ps.[28] The similarity of these efficiencies implies that Auger recombination does not play a large role in an infilled PbSe-EDT QD solid. Escape of charges from Auger recombination in the infilled PbSe-EDT QD solid is facilitated by the high charge mobility of ~2 $cm^2\ V^{-1}\ s^{-1}$ (see Supporting Information, Note 2 for mobility determination).

In conclusion, we show an activation of CM in PbSe-EDT QD solids by ALD infilling with Al_2O_3 or Al_2O_3/ZnO. The yield of free charges produced via CM is close to the yield of electron−hole pairs reported for dispersed PbSe QDs.[4] In the infilled films, Auger recombination does not severely limit the formation of multiple free electrons and holes by a single photon.

METHODS

QD Synthesis. PbSe QDs were synthesized and purified using standard air-free techniques. In a typical synthesis, a solution of 1.09 g PbO (4.9 mmol), 3.45 g oleic acid (12.2 mmol), and 13.5 g 1-octadecene was degassed in a three-neck flask and heated at 180 °C for 1 h to dissolve the PbO and dry the solution. Fifteen milliliters of a 1 M solution of trioctylphosphine selenide containing 0.14 g diphenylphosphine (0.75 mmol) was then rapidly injected into this hot solution. The QDs were grown for 1 min, and the reaction was then quenched with a water bath and 20 mL of anhydrous hexane. The QDs were purified by three rounds of dispersion/precipitation in hexane/ethanol and stored in a glovebox as a powder. The particle size and size distribution were determined from transmission electron microscopy images of at least 100 QDs.

QD Film Preparation. PbSe QD solids were prepared via layer-by-layer dip coating using a mechanical dip coater mounted inside of a glovebox (DC Multi-4, Nima Technology). Quartz substrates were cleaned by subsequently sonicating in acetone, rinsing with acetone and isopropanol and drying under an N_2 flow. Clean substrates were alternately dipped into a 2 mg mL^{-1} dispersion of QDs in dry hexane and then a 1 mM solution of EDT in dry acetonitrile. Resulting QD solids have a $1S_h1S_e$ absorption peak at 1930 nm (0.64 eV; see Figure S1).

Atomic Layer Deposition Infilling. This procedure is detailed elsewhere.[18] Briefly, the interstitial space of a PbSe-EDT QD solid was infilled with amorphous Al_2O_3 (for some samples followed by crystalline ZnO) using low-temperature ALD. This improves carrier mobility and environmental stability of the QD solids. Al_2O_3 was deposited by ALD of trimethylaluminum and water, and ZnO was deposited by ALD of diethylzinc and water. A substrate temperature of 75 °C, pulse (purge) duration of 20 ms (90−120 s), and operating pressure of ~2×10^{-4} bar were used. Synthesis of a 25 nm ALD film requires ~9 h with these parameters.

Steady-State Optical Absorption. Absorption spectra were measured with a Perkin−Elmer Lambda 900 spectrometer equipped with integrating sphere. Infilled films were measured in air inside the integrating sphere. The noninfilled film was kept under N_2 atmosphere. The absorption spectrum of this film was obtained from the measured transmission and reflection spectrum. The band gap energy of the QD solid, E_g, is taken as that photon energy at which the lowest-energy absorption peak shows a maximum.

Time Resolved Microwave Conductivity. Photoconductivity was measured using the time-resolved microwave conductivity technique.[22,23] Samples were mounted in an N_2-filled microwave cavity (8.5 GHz resonance frequency) at the position of maximum electric field (~100 V cm^{-1}). This limits the time resolution to 16 ns due to the response time of the cavity. However, transients were deconvolved for the known cavity response function (see Supporting Information, Note 2), resulting in a time resolution limited by the 3 ns laser pulse. Samples were photoexcited at a 10 Hz repetition rate using 3 ns pulses of tunable wavelength obtained by pumping an optical parametric oscillator with the third harmonic (355 nm) of a Q-switched Nd:YAG laser (Opotek Vibrant 355 II). The laser has a wavelength accuracy of ±5 nm (determined at 1000 nm). An excitation fluence of 2×10^{-4} photons per QD was found to be sufficiently low that higher-order Auger recombination of electrons and holes was insignificant. This fluence was determined as $I_i(1 - F_R)\sigma$, with I_i the incident excitation fluence, F_R the fraction of incident light reflected by the film surface, and σ the absorption cross section[11] of a PbSe QD in dispersion.

The product of the mobility μ and time-dependent yield of mobile charge carriers per absorbed photon $\phi(t)$, summed for photogenerated electrons and holes, is related to the change in probe power P as

dx.doi.org/10.1021/jz4007492 | J. Phys. Chem. Lett. 2013, 4, 1766−1770

$$\phi_e(t)\mu_e + \phi_h(t)\mu_h = -\frac{1}{eK\beta I_0 F_A}\left(\frac{P_{on}(t) - P_{off}}{P_{off}}\right)$$

with t the pump−probe delay time, e the elementary charge, K the frequency-dependent sensitivity factor,[29] β = 2.08 the aspect ratio of the rectangular waveguide, I_0 the fluence incident on the sample, F_A the fraction of photons absorbed by the sample, P_{on} the microwave probe power after passing through the photoexcited sample, and P_{off} the microwave probe power after passing through the ground-state sample. The yield per incident photon η is related to the yield per absorbed photon ϕ as $\eta = \phi F_A$. The MFCG efficiency is determined from the increase of the quantum yield ϕ with photon energy. Hence a constant fraction of charge trapping does not lead to misinterpretation of the efficiency, which is not the case[30] for ultrafast transient absorption experiments employing the peak−tail method.

■ ASSOCIATED CONTENT

Supporting Information

Steady-state absorption spectra and electronic transition energy determination; deconvolution of microwave conductivity transients and determination of lower limit to charge mobility; chemicals used. This material is available free of charge via the Internet at http://pubs.acs.org.

■ AUTHOR INFORMATION

Corresponding Author

*E-mail: L.D.A.Siebbeles@tudelft.nl.

Author Contributions

S.T.C. performed the time-resolved microwave conductivity and steady-state absorption experiments, analyzed the data, and wrote the manuscript. Y.L. synthesized the QDs, prepared the QD solids, and performed the ALD infilling. C.S.S.S. provided the absorption and photoconductivity spectrum of a PbSe-EDT film. S.K. was involved in directing the research. A.J.H. advised on the interpretation. T.J.S. designed the time-resolved microwave conductivity experiment. J.M.S. advised on the experimental work. M.L. and L.D.A.S. designed and supervised the project and edited the manuscript. All authors discussed the results and implications and commented on the manuscript at all stages.

Notes

The authors declare no competing financial interest.

■ ACKNOWLEDGMENTS

This work is part of the Joint Solar Programme (JSP) of Hyet Solar and the Stichting voor Fundamenteel Onderzoek der Materie (FOM), which is part of the Nederlandse Organisatie voor Wetenschappelijk Onderzoek (NWO). C.S.S.S. acknowledges financial support by Toyota Motor Europe NV/SA. L.D.A.S. acknowledges financial support by the 3TU Centre for Sustainable Energy Technologies (Federation of the Three Universities of Technology in The Netherlands). Y.L. and M.L. acknowledge financial support by the Center for Advanced Solar Photophysics (CASP), an Energy Frontier Research Center funded by the U.S. Department of Energy (DOE), Office of Science, Office of Basic Energy Sciences (BES).

■ REFERENCES

(1) Ip, A. H.; Thon, S. M.; Hoogland, S.; Voznyy, O.; Zhitomirsky, D.; Debnath, R.; Levina, L.; Rollny, L. R.; Carey, G. H.; Fischer, A.; et al. Hybrid Passivated Colloidal Quantum Dot Solids. *Nat. Nanotechnol.* **2012**, *7*, 577−582.

(2) Nozik, A. J.; Beard, M. C.; Luther, J. M.; Law, M.; Ellingson, R. J.; Johnson, J. C. Semiconductor Quantum Dots and Quantum Dot Arrays and Applications of Multiple Exciton Generation to Third-Generation Photovoltaic Solar Cells. *Chem. Rev.* **2010**, *110*, 6873−6890.

(3) Hillhouse, H. W.; Beard, M. C. Solar Cells from Colloidal Nanocrystals: Fundamentals, Materials, Devices, and Economics. *Curr. Opin. Colloid Interface Sci.* **2009**, *14*, 245−259.

(4) Beard, M. C.; Luther, J. M.; Semonin, O. E.; Nozik, A. J. *Acc. Chem. Res.* **2012**, DOI: 10.1021/ar3001958.

(5) Beard, M. C. Multiple Exciton Generation in Semiconductor Quantum Dots. *J. Phys. Chem. Lett.* **2011**, *2*, 1282−1288.

(6) Nair, G.; Chang, L. Y.; Geyer, S. M.; Bawendi, M. G. Perspective on the Prospects of a Carrier Multiplication Nanocrystal Solar Cell. *Nano Lett.* **2011**, *11*, 2145−2151.

(7) Beard, M. C.; Ellingson, R. J. Multiple Exciton Generation in Semiconductor Nanocrystals: Toward Efficient Solar Energy Conversion. *Laser Photonics Rev.* **2008**, *2*, 377−399.

(8) McGuire, J. A.; Joo, J.; Pietryga, J. M.; Schaller, R. D.; Klimov, V. I. New Aspects of Carrier Multiplication in Semiconductor Nanocrystals. *Acc. Chem. Res.* **2008**, *41*, 1810−1819.

(9) Nozik, A. J. Multiple Exciton Generation in Semiconductor Quantum Dots. *Chem. Phys. Lett.* **2008**, *457*, 3−11.

(10) Hanna, M. C.; Nozik, A. J. Solar Conversion Efficiency of Photovoltaic and Photoelectrolysis Cells with Carrier Multiplication Absorbers. *J. Appl. Phys.* **2006**, *100*, 074510.

(11) Moreels, I.; Lambert, K.; De Muynck, D.; Vanhaecke, F.; Poelman, D.; Martins, J. C.; Allan, G.; Hens, Z. Composition and Size-Dependent Extinction Coefficient of Colloidal PbSe Quantum Dots. *Chem. Mater.* **2007**, *19*, 6101−6106.

(12) Trinh, M. T.; Polak, L.; Schins, J. M.; Houtepen, A. J.; Vaxenburg, R.; Maikov, G. I.; Grinbom, G.; Midgett, A. G.; Luther, J. M.; Beard, M. C.; et al. Anomalous Independence of Multiple Exciton Generation on Different Group IV-VI Quantum Dot Architectures. *Nano Lett.* **2011**, *11*, 1623−1629.

(13) Trinh, M. T.; Houtepen, A. J.; Schins, J. M.; Hanrath, T.; Piris, J.; Knulst, W.; Goossens, A. P. L. M.; Siebbeles, L. D. A. In Spite of Recent Doubts Carrier Multiplication Does Occur in PbSe Nanocrystals. *Nano Lett.* **2008**, *8*, 1713−1718.

(14) Ellingson, R. J.; Beard, M. C.; Johnson, J. C.; Yu, P. R.; Micic, O. I.; Nozik, A. J.; Shabaev, A.; Efros, A. L. Highly Efficient Multiple Exciton Generation in Colloidal PbSe and PbS Quantum Dots. *Nano Lett.* **2005**, *5*, 865−871.

(15) Gao, Y. N.; Aerts, M.; Sandeep, C. S. S.; Talgorn, E.; Savenije, T. J.; Kinge, S.; Siebbeles, L. D. A.; Houtepen, A. J. Photoconductivity of PbSe Quantum-Dot Solids: Dependence on Ligand Anchor Group and Length. *ACS Nano* **2012**, *6*, 9606−9614.

(16) Liu, Y.; Gibbs, M.; Puthussery, J.; Gaik, S.; Ihly, R.; Hillhouse, H. W.; Law, M. Dependence of Carrier Mobility on Nanocrystal Size and Ligand Length in PbSe Nanocrystal Solids. *Nano Lett.* **2010**, *10*, 1960−1969.

(17) Ihly, R.; Tolentino, J.; Liu, Y.; Gibbs, M.; Law, M. The Photothermal Stability of PbS Quantum Dot Solids. *ACS Nano* **2011**, *5*, 8175−8186.

(18) Liu, Y.; Gibbs, M.; Perkins, C.; Tolentino, J.; Zarghami, M.; Bustamante, J.; Law, M. Robust, Functional Nanocrystal Solids by Infilling with Atomic Layer Deposition. *Nano Lett.* **2011**, *11*, 5349−5404.

(19) Miaja-Avila, L.; Tritsch, J. R.; Wolcott, A.; Chan, W. L.; Nelson, C. A.; Zhu, X. Y. Direct Mapping of Hot-Electron Relaxation and Multiplication Dynamics in PbSe Quantum Dots. *Nano Lett.* **2012**, *12*, 1588−1591.

(20) Beard, M. C.; Midgett, A. G.; Law, M.; Semonin, O. E.; Ellingson, R. J.; Nozik, A. J. Variations in the Quantum Efficiency of Multiple Exciton Generation for a Series of Chemically Treated PbSe Nanocrystal Films. *Nano Lett.* **2009**, *9*, 836−845.

(21) Law, M.; Beard, M. C.; Choi, S.; Luther, J. M.; Hanna, M. C.; Nozik, A. J. Determining the Internal Quantum Efficiency of PbSe Nanocrystal Solar Cells with the Aid of an Optical Model. *Nano Lett.* **2008**, *8*, 3904−3910.
(22) Kroeze, J. E.; Savenije, T. J.; Vermeulen, M. J. W.; Warman, J. M. Contactless Determination of the Photoconductivity Action Spectrum, Exciton Diffusion Length, and Charge Separation Efficiency in Polythiophene-Sensitized TiO_2 Bilayers. *J. Phys. Chem. B* **2003**, *107*, 7696−7705.
(23) De Haas, M. P.; Warman, J. M. Photon-Induced Molecular Charge Separation Studied by Nanosecond Time-Resolved Microwave Conductivity. *Chem. Phys.* **1982**, *73*, 35−53.
(24) Aerts, M.; Suchand Sandeep, C. S.; Gao, Y.; Savenije, T. J.; Schins, J. M.; Houtepen, A. J.; Kinge, S.; Siebbeles, L. D. A. Free Charges Produced by Carrier Multiplication in Strongly Coupled PbSe Quantum Dot Films. *Nano Lett.* **2011**, *11*, 4485−4489.
(25) Talgorn, E.; Gao, Y.; Aerts, M.; Kunneman, L. T.; Schins, J. M.; Savenije, T. J.; Van Huis, M. A.; Van der Zant, H. S. J.; Houtepen, A. J.; Siebbeles, L. D. A. Unity Quantum Yield of Photogenerated Charges and Band-Like Transport in Quantum-Dot Solids. *Nat. Nanotechnol.* **2011**, *6*, 733−739.
(26) Gao, Y. N.; Talgorn, E.; Aerts, M.; Trinh, M. T.; Schins, J. M.; Houtepen, A. J.; Siebbeles, L. D. A. Enhanced Hot-Carrier Cooling and Ultrafast Spectral Diffusion in Strongly Coupled PbSe Quantum-Dot Solids. *Nano Lett.* **2011**, *11*, 5471−5476.
(27) Beard, M. C.; Midgett, A. G.; Hanna, M. C.; Luther, J. M.; Hughes, B. K.; Nozik, A. J. Comparing Multiple Exciton Generation in Quantum Dots to Impact Ionization in Bulk Semiconductors: Implications for Enhancement of Solar Energy Conversion. *Nano Lett.* **2010**, *10*, 3019−3027.
(28) Klimov, V. I.; McGuire, J. A.; Schaller, R. D.; Rupasov, V. I. Scaling of Multiexciton Lifetimes in Semiconductor Nanocrystals. *Phys. Rev. B* **2008**, *77*, 195324.
(29) Savenije, T. J.; de Haas, M. P.; Warman, J. M. The Yield and Mobility of Charge Carriers in Smooth and Nanoporous TiO_2 Films. *Z. Phys. Chem. (Muenchen, Ger.)* **1999**, *212*, 201−206.
(30) McGuire, J. A.; Sykora, M.; Joo, J.; Pietryga, J. M.; Klimov, V. I. Apparent Versus True Carrier Multiplication Yields in Semiconductor Nanocrystals. *Nano Lett.* **2010**, *10*, 2049−2057.